Inductance and Torque Characteristics Analysis of Multi-Layer Buried Magnet Synchronous Machines

Sang-Yeop Kwak †, Jae-Kwang Kim* and Hyun-Kyo Jung*

Abstract - Inductance characteristics, torque variations and ripple according to current, and position of multi-layer buried magnet synchronous machines with field-weakening operations are presented. The rotor structure optimal design of a buried magnet synchronous machine with high performance is investigated, and optimization results and comparison among design candidates are shown. For the fast and accurate search of multiple optima, the auto-tuning niching genetic algorithm is used and a final solution is selected considering various design factors.

Keywords: finite element method (FEM), genetic algorithm (GA), inductance, interior permanent magnet synchronous motor (IPMSM)

1. Introduction

The interior permanent magnet synchronous motor (IPMSM) has many advantages, such as high efficiency, high power density, high torque density and a wide speed range among others, because the motor can utilize both magnet and reluctance torque due to the magnetic saliency [1-3]. In recent years, with developments in power electronics and improvements in permanent magnet performance, the IPMSM has been widely used for electric household appliances and special machines such as the integrated starter/generator (ISG) for electric vehicles [4-7]. In particular, the characteristics such as high efficiency, high torque and wide constant power speed range are required for ISG, and the IPMSM, which uses field-weakening control, satisfies these demands [4]. However, there exists a discrepancy between the experimental data and the calculation results in research on the characteristic analysis and optimal design of the multi-layer buried magnet synchronous machine.

In this paper, the inductance and torque analysis of multi-layer buried magnet synchronous motors using the finite element method has been presented. Phase inductance variation aspect according to rotor position indicates that it is difficult to accurately analyze the influence of magnet flux. Due to saturation and leakage flux, it is erroneous to treat the magnet flux constant as irrelevant to rotor position. If inaccurate inductance is obtained by calculation, it is impossible to use vector control based on dq-transformation. Therefore, a new calculation method considering the non-linearity of magnet flux including saturation and leakage effect is needed. Meanwhile, by the investigation of torque variation according to rotor position, an analysis of maximum torque and torque ripple is performed.

Moreover, auto-tuning niching GA is used for the optimal design of IPM rotor structure and results of optimization are presented. The population size and niche radii can be determined automatically in this algorithm, and so it is possible to search multiple solutions fast and accurately without previous information. Some types of rotor structures are presented and their optimal design is executed. It has been demonstrated that there are several good solutions for the problems, such as shape or structural optimization of an electromagnetic device.

2. Analysis Model and Application Requirements

The IPMSM in this paper will be applied to the integrated starter/generator (ISG), which requires significant starting torque and a wide constant power speed range, and is driven by an inverter and a low voltage (42[V]) battery. Since magnets are buried in the rotor core, the dispersion of the magnet is obviously minimized, and IPMSMs also have the advantage of additional reluctance torque. Due to these and other refinements, IPMSMs are widely considered to be suitable for high-speed operation, and have been known to have better power density than other PM machines. For high power density, flux-weakening control is essential for stable operation in the wide constant power speed range, and the increase of rotor saliency is very important [8]. Back-emf limit in the high-speed range and battery operation must be considered

† Corresponding Author: School of Electrical Engineering, Seoul National University, Korea. (aceonepair@elecmech.snu.ac.kr)
* School of Electrical Engineering, Seoul National University, Korea.
Received May 6, 2004 ; Accepted August 31, 2004

together for ISG application. Therefore, ferrite magnets, which have the advantage of small residual flux density, are a good choice in this.

Design specification is summarized in Table 1 and, as shown in Fig. 1, magnet layers block the d-axis magnetic flux path in the rotor structure. Therefore, the q-axis inductance (L_{qs}) is greater than the d-axis inductance (L_{ds}), and the inductance difference of the two axes has been used with advantage for the attainment of high capability and extended speed range of motor operation.

Application requirements of Fig. 2(b) indicate that high starting torque and wide constant speed range are needed. It is easy to extend the constant power region of Fig. 2(a) in case of IPMSM with facile flux-weakening operation.

Table 1 Specifications of analysis model

Parameters and constraints	value
Pole number	8
Outer diameter of the rotor	200 mm
Inner diameter of the rotor	116.2 mm
Air gap	0.7 mm
Inner diameter of the stator	201.4 mm
Outer diameter of the stator	270 mm
Stacking depth	70 mm
Number of slot	48
Permanent magnet	Ferrite magnet (Br = 3700 Gauss)
Current density (at 500 Apeak)	$26.2A_{rms}/mm^2$
Fill factor	45.7 %
KE	0.01226 V_{peak}/rad/sec
Per phase winding resistance	8.4 mΩ

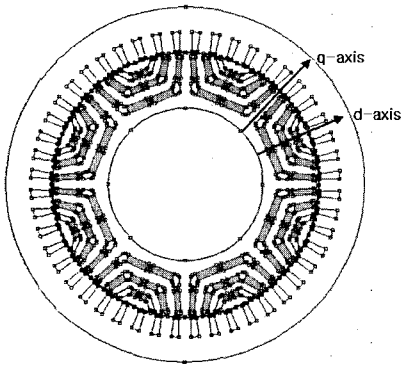

Fig. 1 Analysis model

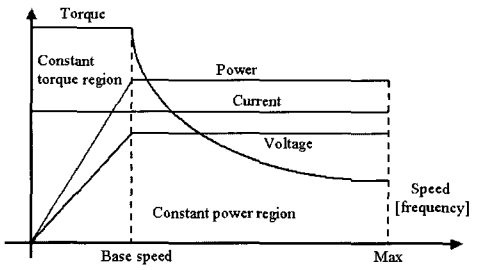

(a)

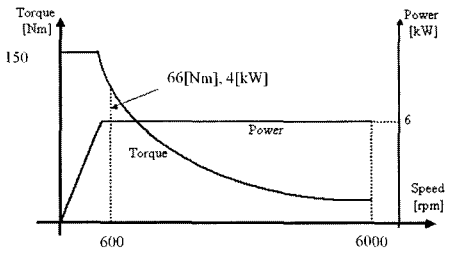

(b)

Fig. 2 Speed-Torque characteristic curves (a) and application requirements (b)

3. Inductance and Torque Characteristics

3.1 Inductance Characteristics

Design and performance evaluations using d or q-axis inductance are based on the dq-transformation derived in [9]. The self-inductance of each phase is as follows.

$$L_{aa} = L_0 - L_2 \cos 2\theta_r \tag{1}$$

$$L_{bb} = L_0 - L_2 \cos(2\theta_r + 2\pi/3) \tag{2}$$

$$L_{cc} = L_0 - L_2 \cos(2\theta_r - 2\pi/3) \tag{3}$$

where θ_r is the electrical degree. If the self-inductance of each phase has an ideal sine waveform and total leakage flux is slight, the inductances of the d-axis and the q-axis are derived like this.

$$L_{ds} = \frac{3}{2}(L_0 - L_2) \tag{4}$$

$$L_{qs} = \frac{3}{2}(L_0 + L_2) \tag{5}$$

where $L_0 = 2L_2$ is the average value of self-inductance defined in [9].

For computing the L_{aa} using FEM, the effect of PM-induced magnetic flux is considered linearly and, that is to say, the flux linkage due to current is derived with the subtraction of the flux linkage without winding excitation from the flux linkage with double excitation. Fig. 4 depicts the result of L_{aa} analysis. We can see that the inductance of the a-phase does not have an ideal sine waveform, and the variation aspect is different, due to the stator current. Considering saturation effects resultant from high current density, q-axis inductance is independent of rotor position (0° and 180°). Conversely, d-axis inductance is dependent

on rotor position (90° and 270°).

As previously mentioned, in conventional FE analysis, PM flux-linkage is subtracted linearly from the total PM flux-linkage and stator current for the inductance calculation. This means that PM flux-linkage according to rotor position is assumed to be constant, and irrelevant to stator current. However, as shown in Fig. 3, saturation effects dramatically increase with high stator current, and PM flux-linkage varies according to stator current. Therefore, the mismatch between the calculated inductance by this method and the experimental one is observed as shown in Fig. 4, and it is not suitable to utilize (4) and (5) for estimating L_{ds} and L_{qs} under the operating point.

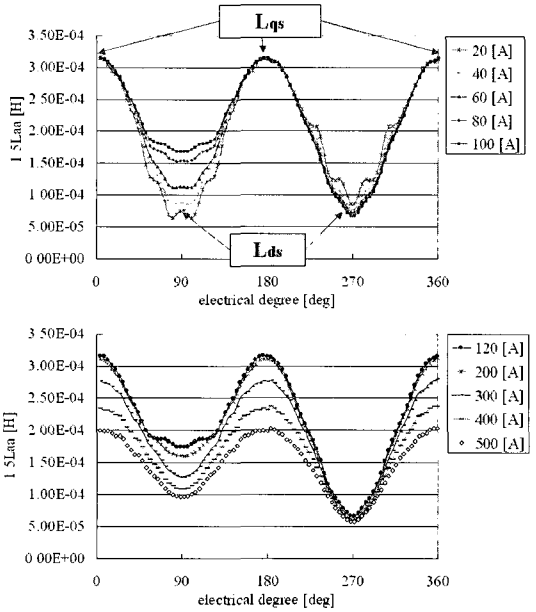

Fig. 3 The calculated a-phase inductance (L_{aa}) of analysis model (by FEM)

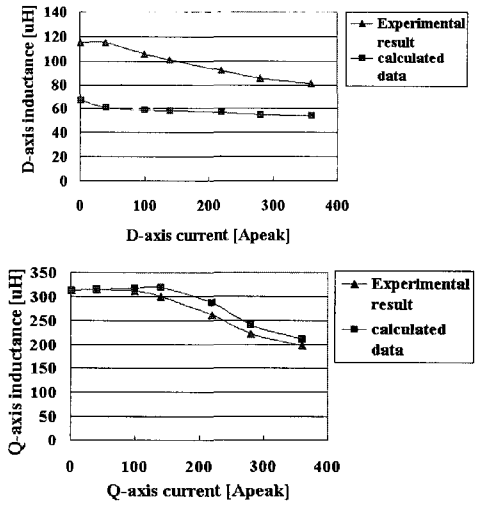

Fig. 4 The calculated and experimental inductance of d-axis and q-axis of the analysis model

3.2 Torque Characteristics

Smooth torque curve as well as accurate d-axis and q-axis inductances is essential for precise vector control. Torque analysis results using the finite element method suggest that there torque ripple is significant (20~30[%]) as shown in Fig. 5(b). Therefore, it is essential to reduce torque ripple using the optimization methods for applying vector control. With the increase of current, the rotor position generating maximum torque per unit current changes as shown in Fig. 5(a) and this position is affected by various reasons such as slot, teeth and structure of the rotor.

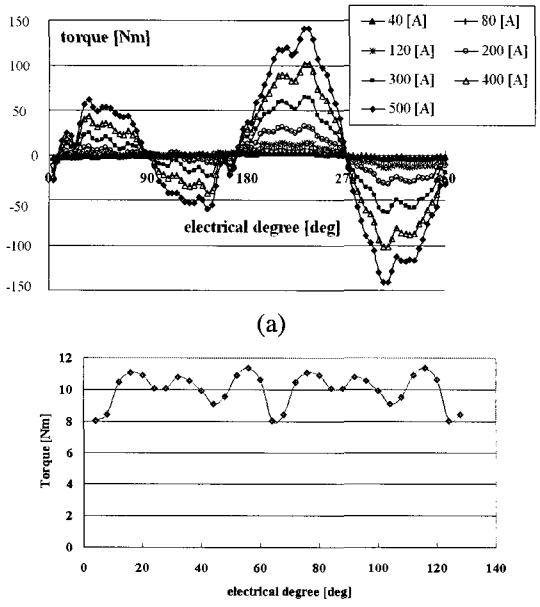

Fig. 5 Torque characteristics of analysis model (by FEM) (a) Torque vs. rotor position (b) Torque ripple (current: 100[A])

4. Optimal Design of Rotor Configuration

The sample model in this paper is a multi-layer buried magnet synchronous machine with high performance. The initial shape of the sample model is depicted in Fig. 6. The sample model has a basic structure of 4 poles, two-layer magnet rotor, 36 slots, short pitch distribution winding, and is driven by an inverter. The bridge in Fig. 1 has at least 1[mm] thickness for the prevention of the dispersion of magnets due to the centrifugal force inherent in the high-speed region (over 18000[rpm]). Because the increase of bridge thickness leads to a drop in efficiency due to increment of flux leakage, the thickness of the bridge is fixed (1[mm]).

To satisfy the required performance (starting torque,

generating power and back-emf limit) presented in Table 2, an optimal design of the rotor structure (magnet dimension) is fulfilled. In this paper, the auto-tuning niching genetic algorithm combined with the pattern search method is used as an optimization method to perform a fast and accurate search [10, 11]. This is a genetic algorithm automatically determining the population size and niche radii. The flowchart of the auto-tuning niching genetic algorithm is indicated in Fig. 7.

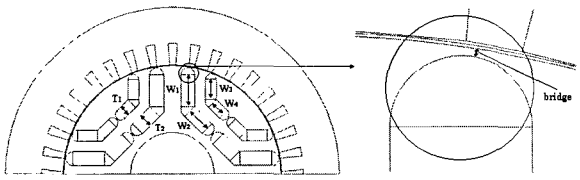

Fig. 6 Sample model (IPMSM)

Table 2 Design specifications of analysis model

	Quantity	Value	Unit
Dimension	Inner radius of rotor	20	mm
	Outer radius of rotor	60	mm
	Airgap	0.7	mm
	Inner radius of stator	60.7	mm
	Outer radius of stator	95	mm
	Width of teeth	7	mm
Magnetic circuit	Magnetic remanence	3700	G
	Coercive force	2950	Oe
Driver	Motoring torque (starting)	150	Nm
	Generating power (1800[rpm])	4000	W
	Generating power (18000[rpm])	6000	W
	Back-emf limit	52	V

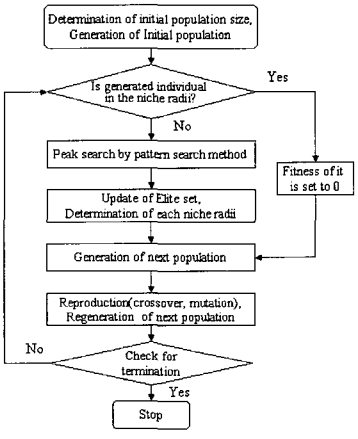

Fig. 7 Flowchart of auto-tuning niching genetic algorithm.

In this algorithm, multiple optima can be searched by the elitism and niche concept, and each optimum can be searched quickly and accurately by combination niching GA and pattern search method. Starting torque is used as the objective function and generating power can be taken into account by post-process. Starting torque and generating power can be obtained by FEA. If magnet residual flux density, the number of slots, air gap length, the number of stator turns, stator bore, stator yoke depth, stator slot depth, and stator outer radius are assumed to be constant values, the thickness and width of each magnet as shown in Fig. 6 (T1, T2, W1, W2, W3, W4) are chosen as the design variables.

5. Optimization Results

Four representative results of optimal design by the auto-tuning niching genetic algorithm are shown in Fig. 8 and Table 3. In the optimization process of the two-layer magnet rotor structure (no spoke-type), candidates 1 and 2 are obtained. In the case of candidate 1, optimal design of a two-layer spoke-type rotor structure is performed and candidates 3 and 4 are obtained. In the case of candidates 3 and 4, W2 can be determined by W1. Because of space limitations, the stator outer radius of each candidate is assumed to be constant. Therefore by adjusting the stacking length of each candidate, the starting torque of each candidate becomes 150 [Nm]. Though there is disparity between the stacking length of candidates 1, 3 and 4, it is very small (under 10[%]).

Table 3 Optimal design result and design candidates

	T_1 [mm]	T_2 [mm]	W_1 [mm]	W_2 [mm]	W_3 [mm]	W_4 [mm]
Candidate 1	6.0	8.2	21.9	11	8.8	5.5
Candidate 2	6.1	7.9	17.2	7.3	9.0	5.7
Candidate 3	5.8	8.0	19.8		9.25	6.1
Candidate 4	6.0	8.1	22.7		7.5	6.2

Table 4 Characteristics of design candidates

	Starting Torque	Stacking length	Stress
Candidate 1	150 [Nm]	77 [mm]	Normal
Candidate 2	150 [Nm]	86 [mm]	Good
Candidate 3	150 [Nm]	74 [mm]	Normal
Candidate 4	150 [Nm]	72 [mm]	Bad

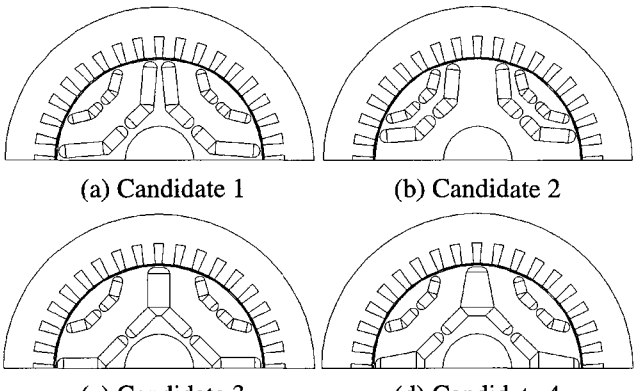

(a) Candidate 1 (b) Candidate 2

(c) Candidate 3 (d) Candidate 4

Fig. 8 Optimization results

If the feasibility of the manufacturer, stacking length, stress and design experienced are considered together, candidate 3 with larger stacking length than candidate 4 can be selected for the best solution.

6. Conclusion

Analysis results of inductance and torque characteristics of IPMSM with high performance are presented. Non-linearity of inductance variation and maximum torque operation per unit current according to rotor position are investigated closely and, therefore, a new analytic approach is required to consider the notable influence by the large input current and the non-linear (saturation) effect in ferromagnetic material in the next research aim.

Meanwhile, rotor structure optimization of the buried magnet synchronous machine with high performance is investigated. The objective function is starting torque, and the design variables are the dimensions related to the rotor structure of the sample model (IPMSM). Four representative candidates are obtained by auto-tuning the niching genetic algorithm that can search multiple solutions fast and accurately without previous information. By considering basic characteristics, feasibility, and design experience collectively, the final optimal solution is determined.

References

[1] T.J.E.Miller, Brushless Permanent Magnet and Reluctance Motor Drives, Oxford, 1989.

[2] P. Pillay, et al., Performance & Design of Permanent Magnet AC Motor Drives, IEEE IAS tutorial course, 1991.

[3] N.Bianchi, S.Bolognani, "Interior PM Synchronous Motor for High Performance Applications," *PCC-Osaka 2002,* Proceedings of the, Vol. 1, pp. 148-153, 2002.

[4] J. F. Gieras, E. Santini, and M. Wing, "Calculation of synchronous reactances of small permanent-magnet alternating-current motors: comparison of analytical approach and finite element method with mesurement," *IEEE Trans. Magn.,* Vol. 34, pp. 3712-3720, Sept. 1998.

[5] C.Mademlis, V.G.Agelidis, "A High-Performance Vector Controlled Interior PM Synchronous Motor Drive with Extended Speed Range Capability," IECON'01, Vol. 2, pp. 1475-1482, 2001.

[6] Soong.W.L., Ertugrul.N., Lovelace.E.C., Jahns.T.M., "Investigation of interior permanent magnet offset-coupled automotive integrated starter/alternator," *Industry Applications Conference, 2001. Thirty-Sixth IAS Annual Meeting*, Vol. 1, pp. 429–436, 2001.

[7] Lovelace.E.C., Keim.T., Lang.J.H., Wentzloff.D.D., Jahns.T.M., Wai. J., McCleer.P.J., "Design and experimental verification of a direct-drive interior PM synchronous machine using a saturable lumped-parameter model," *Industry Applications Conference 2002. 37th IAS Annual Meeting*, Vol. 4, pp. 2486-2492, Oct. 2002.

[8] Bon-Ho Bae, Seung-Ki Sul, "Practical design criteria of interior permanent magnet synchronous motor for 42V integrated starter-generator," *Electric Machines and Drives Conference, 2003. IEMDC'03. IEEE International*, Vol. 2, pp. 656-662, 2003.

[9] J.Wai, T.M.Jahns, "A New Control Technique for Achieving Wide Constant Power Speed Operation with an Interior PM Alternator Machine," *IAS Annual Meeting 2001*, Vol. 2, pp. 807-814, 2001.

[10] Paul C. Krause, Analysis of Electric Machinery, pp. 36-54, IEEE PRESS, 1995.

[11] Dong-Hyeok Cho, Hyun-Kyo Jung, Cheol-Gyun Lee, "Niching Genetic Algorithm Adopting Restricted Competition Selection Combined with a Deterministic Method," *CEFC-2000*, p.337, June 4-7, 2000.

[12] S.W. Mahfoud, *Niching Methods for Genetic Algorithms,* Doctoral Dissertation / IlliGAL Report 95001, University of Illinois at Urbana-Champaign, Illinois Genetic Algorithm Laboratory, 1995.

Sang-Yeop Kwak

He received his B.S. and M.S. degrees in Electrical Engineering from Seoul National University, Seoul, Korea, in 2002 and 2004, respectively, and is currently working toward his Ph.D. degree at the same institution. His current research is focused on the design and characteristics analysis of interior permanent magnet synchronous machines.

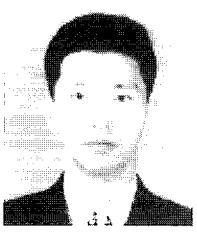

Jae-Kwang Kim

He received his B.S. and M.S. degrees in Electrical Engineering from Seoul National University, Seoul, Korea, in 1999 and 2001, respectively, and is currently working toward his Ph.D. degree at the same institution. His current research is focused on the design and characteristics analysis of interior permanent magnet synchronous machines.

Hyun-Kyo Jung

He received his B.S., M.S., and Ph.D. degrees in Electrical Engineering from Seoul National University, Seoul, Korea, in 1979, 1981, and 1984, respectively. He is currently a Professor with the School of Electrical Engineering and Computer Science /Electrical Engineering, Seoul National University. His research interests are various fields of the analysis and design of electric machines and numerical analysis of electrical systems, especially with the FEM.